

# Compressed Ethylene-Assisted Formation of the Reverse Micelle of PEO–PPO–PEO Copolymer

Rui Zhang,<sup>†</sup> Jun Liu,<sup>†</sup> Jun He,<sup>†</sup> Buxing Han,<sup>\*,†</sup> Zhimin Liu,<sup>†</sup> Tao Jiang,<sup>†</sup> Weize Wu,<sup>†</sup> Lixia Rong,<sup>‡</sup> Hui Zhao,<sup>‡</sup> Baozhong Dong,<sup>‡</sup> and Guo-Hua Hu<sup>\*,§</sup>

The Center for Molecular Sciences, Institute of Chemistry, Chinese Academy of Sciences, Beijing 100080, China; Institute of High Energy Physics, Chinese Academy of Sciences, Beijing 100039, China; and Laboratory of Chemical Engineering Sciences, CNRS-ENSIC-INPL, 54001 Nancy Cedex, France

Received September 6, 2002; Revised Manuscript Received December 5, 2002

**ABSTRACT:** The triblock copolymer (EO)<sub>27</sub>(PO)<sub>61</sub>(EO)<sub>27</sub> aggregates in *p*-xylene upon addition of ethylene. An abrupt increase of water solubilization is observed at a certain ethylene pressure. The molar ratio of water to EO segment ( $W_0$ ) can be as high as 4.2 under suitable conditions. The reverse micelles can solubilize ionic substances, such as methyl orange. The polarity of the water domains increases with increasing  $W_0$  as shown by a solvatochromic study. The structure of the reverse micelles is characterized by small-angle X-ray scattering and Fourier transform infrared. The results indicate the existence of lamellar structure and “bulk” (hydrogen-bonded) water (H<sub>2</sub>O and D<sub>2</sub>O) in the reverse micellar system. The formation and breaking of the reverse micelles can be repeated by adjusting the ethylene pressure.

## Introduction

Surfactants self-assemble in solutions and thus enhance compatibility or segregation between immiscible solvents.<sup>1</sup> The resulting systems, clear and thermodynamically stable, are normally known as micelle solutions or microemulsions.<sup>2</sup> Such micelles or microemulsions have been successfully used in many fields, such as separation and extraction of proteins<sup>3</sup> and as nano-reactors for enzymatic or catalytic reactions.<sup>4–6</sup>

Block copolymers can also self-assemble in selective solvents.<sup>7,8</sup> Amphiphilic block copolymers, known as poloxamers, which contain hydrophilic poly(ethylene oxide) (PEO) and hydrophobic poly(propylene oxide) (PPO) blocks, are commercially available and widely used recently. They can form normal micelles (with a “core” of water-insoluble PPO and a “corona” composed by the water-soluble PEO blocks) in aqueous solution.<sup>9</sup> These copolymers can also form reverse micelles in some organic solvents, such as *o*-xylene and *p*-xylene.<sup>10–12</sup>

In addition to being controlled by the chemistry (e.g., copolymer composition and molecular mass) and the amphiphilic character of the polymer, the formation of micelles can be modulated by physical means, such as by altering the interactions between the blocks of polymer and the aqueous and/or organic solvents.<sup>12</sup> The solvent property has a great effect on the formation of the micelles. An increase in temperature or the presence of added salts has a marked influence on critical micelle concentrations (cmc), micelle structures, and micellar parameters of PEO–PPO–PEO copolymer surfactants in both aqueous and organic solvents.<sup>12–14</sup>

Compressed gases, such as CO<sub>2</sub> and ethylene, are quite soluble in a number of organic solvents and lead to their expansion. The solvent strength of the gas-

expanded liquid can be reduced to such an extent that solutes dissolved in the pure liquid can precipitate because the compressed gas is poor solvent for the solutes. This process is often referred to as the gas antisolvent process (GAS).<sup>15,16</sup> GAS techniques have been used in different fields, such as polymer fractionation,<sup>17</sup> recrystallization,<sup>18</sup> and particle generation.<sup>19</sup> It is attractive to tune the solvent strength with gas antisolvent because the process is reversible, the gas is completely separated from the solvent after depressurizing, and the recycling of the gas can be easily achieved. With the gas-expanded solvent, it is possible to achieve an optimum condition for some processes or reactions.<sup>20</sup>

In the previous communication,<sup>21</sup> we reported that the compressed CO<sub>2</sub> could enhance formation of reverse micelles of the (EO)<sub>27</sub>(PO)<sub>61</sub>(EO)<sub>27</sub> copolymer in *p*-xylene,<sup>21</sup> and the reverse micelles formed in CO<sub>2</sub>-expanded *p*-xylene can solubilize a significant amount of water and ionic chemicals. However, some very interesting questions need to be studied further. For example, besides CO<sub>2</sub>, can other gases induce the formation of the reverse micelles? What is the structure of the reverse micelles? Why can the gas enhance the formation of the reverse micelles? Here, we study the enhancement of the reverse micelle by ethylene. The structure of the reverse micelles is characterized by using small-angle X-ray scattering (SAXS) and Fourier transform infrared (FTIR) spectroscopy, which cannot be used with CO<sub>2</sub> because the IR absorption bands of water and CO<sub>2</sub> overlap. The possible mechanism of the formation of the reverse micelles induced by the gases is also discussed.

## Experimental Section

**Materials.** Pluronic P104 was provided by BASF Corp. with a composition of (EO)<sub>27</sub>(PO)<sub>61</sub>(EO)<sub>27</sub>. Methyl orange (MO) was produced by Beijing Chemical Reagent Factory (A.R. Grade). *p*-Xylene was purchased from Beijing Fuxing Chemical Reagent Factory (A.R. Grade). Ethylene (99.9% purity) was supplied by Beijing Analytical Instrument Factory. Double distilled water was used.

<sup>†</sup> Institute of Chemistry, Chinese Academy of Sciences.

<sup>‡</sup> Institute of High Energy Physics, Chinese Academy of Sciences.

<sup>§</sup> CNRS-ENSIC-INPL.

\* Corresponding authors: e-mail hanbx@infoc3.icas.ac.cn or hu@ensic.inpl-nancy.fr.

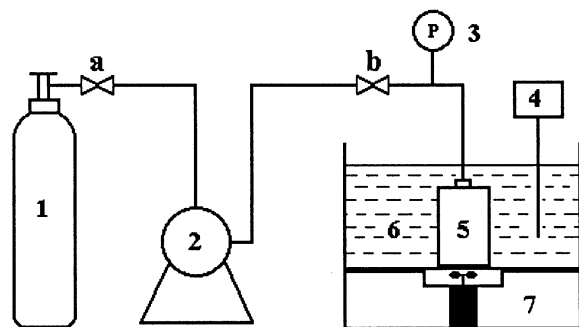


**Figure 1.** Schematic diagram of the apparatus for studying the solubilization of water: 1, gas cylinder; 2, high-pressure syringe pump; 3, pressure gauge; 4, temperature controller; 5, high-pressure view cell; 6, water bath; 7, magnetic stirrer; a and b, valves.

**Apparatus and Procedures To Determine Water Solubilization.** The experiments are based on the fact that the solution is clear and transparent only if the water is all solubilized.<sup>11,12</sup> The apparatus to study water solubilization and volume expansion coefficient of  $\text{H}_2\text{O}/\text{P104}/p\text{-xylene/ethylene}$  quaternary system is same as that used previously.<sup>21</sup> The schematic diagram of the apparatus is shown in Figure 1. It consisted mainly of a high-pressure view cell with a volume of  $40\text{ cm}^3$ , a constant temperature water bath, a high-pressure syringe pump (DB-80), a pressure gauge, a magnetic stirrer, and a gas cylinder. The experimental temperature of the water bath was controlled to  $313.15 \pm 0.05\text{ K}$  by a HAAKE D8 temperature controller. The pressure gauge was composed of a pressure transducer (FOXBORO/ICT, model 93) and an indicator, which was accurate to  $\pm 0.025\text{ MPa}$  in the pressure range  $0\text{--}20\text{ MPa}$ .

In a typical experiment, a  $5\text{ g}$  solution of P104 in  $p\text{-xylene}$  and the desired amount of double distilled water was loaded into the high-pressure view cell. The cell was placed into the constant temperature water bath. After thermal equilibrium had been reached, the stirrer was started and the solution was hazy and milky. Gaseous ethylene was charged into the cell slowly until the hazy and milky solution became transparent and completely clear, indicating the complete solubilization of the water.<sup>11,12</sup>

**UV-vis Experiment.** The solubilization of MO in the reverse micelles was studied by UV-vis spectroscopy. The apparatus and the procedures were similar to those reported previously.<sup>21</sup> It consisted of a gas cylinder, a high-pressure pump, a pressure gauge, an UV-vis spectrometer, a temperature-controlled high-pressure UV sample cell, and valves and fittings. The UV-vis spectrophotometer was produced by Beijing General Instrument Co. (model TU-1201, resolution  $0.1\text{ nm}$ ). The sample cell was composed mainly of a stainless steel body, two quartz windows, a stirrer, and a temperature controlling system. The optical path length and the inner volume of the cell were  $1.32$  and  $1.74\text{ cm}^3$ , respectively. In the experiment, the sample cell was flushed with ethylene to remove the air. Desired amounts of MO aqueous solution of suitable concentration and polymer solution in  $p\text{-xylene}$  were charged into the sample cell. After thermal equilibrium had been reached, ethylene was compressed into the UV cell to the desired pressure. The UV spectrum at equilibrium condition was recorded, which was confirmed by the fact that the UV spectra recorded were independent of equilibration time.

**SAXS Experiment.** The setup for the SAXS study was similar to that described previously.<sup>22</sup> Briefly, the apparatus consisted mainly of a gas cylinder, a high-pressure pump, a digital pressure gauge, a high-pressure SAXS cell, a thermometer and temperature controller, and valves and fittings of different kinds. The pressure gauge consisted of a transducer and an indicator as described above. The temperature-controlled SAXS cell was made of stainless steel body with two diamond windows of  $8\text{ mm}$  in diameter and  $0.4\text{ mm}$  in thickness. The cell body was wrapped in an electric heater and

heat insulating tape outside. The X-ray path length of the cell was  $1.5\text{ mm}$ , and the internal volume of the cell was  $2.7\text{ cm}^3$ . A small magnetic stirrer in the cell stirred the fluids before the SAXS experiments. The insulated cell was electrically heated to  $\pm 0.1\text{ K}$  of the desired temperature using a temperature controller with a platinum resistance temperature probe (model XMT, produced by Beijing Chaoyang Automatic Instrument Factory).

SAXS experiments were carried out at Beamline 4B9A at the Beijing Synchrotron Radiation Facility, using a SAXS apparatus constructed at the station. A detailed description of the spectrometer was given elsewhere.<sup>23</sup> The detector can be translated along the vertical and horizontal axes in a range of  $30\text{ mm}$  with a precision of  $10\text{ }\mu\text{m}$ . The experiments had an angular resolution of better than  $0.5\text{ mrad}$  with this setting. The data accumulation time was  $3\text{ min}$ . The angular range was chosen to provide data from  $q = 0.05\text{ nm}^{-1}$  to  $q = 1.5\text{ nm}^{-1}$ , where the magnitude of scattering vector  $q = 4\pi \sin \theta / \lambda$ , with  $2\theta$  and  $\lambda$  being respectively the scattering angle and incident X-ray wavelength of  $0.154\text{ nm}$ . The distance between the sample chamber and the detector was  $1.470\text{ m}$ . Background scattering from the slit collimator, the solvent, and the residual air path between the vacuum chamber and the detector was measured and subtracted. For each measurement, the solvent with antisolvent ethylene at the same temperature and pressure was used as the background solvent, and in experimental data, the scattering intensity of corresponding background solvent has been subtracted. Excess SAXS scattering from the sample solution was also corrected for incident beam decay and transmission. The SAXS experimental procedure was similar to that for UV-vis measurement described above. The SAXS cell was flushed with ethylene, and then a suitable amount of P104 in  $p\text{-xylene}$  and double distilled water were added to the cell. Ethylene was charged into the cell with stirring after thermal equilibrium had been reached. The cell was connected to the apparatus after the enough equilibration time, and the X-ray scattering was recorded. The pressures investigated were the same as those for phase behavior study.

**FTIR Experiment.** The apparatus and the procedures were similar to those reported previously.<sup>24</sup> It consisted of a gas cylinder, a high-pressure pump, a pressure gauge, an IR spectrometer, a temperature-controlled high-pressure IR sample cell, and valves and fittings. FTIR spectra of all the samples with resolution of  $4\text{ cm}^{-1}$  were taken on a Bruker VECTER 22 FTIR spectrometer using DTGS (deuteriotriglycine sulfate) detector. To obtain a good quality of the spectra,  $64$  scans were accumulated. The sample cell was composed mainly of a stainless steel body, two ZnS windows of  $6\text{ mm}$  thickness, a stirrer, and a temperature controlling system. The optical path length and the inner volume of the cell were  $1.27$  and  $1.32\text{ cm}^3$ , respectively. The insulated cell was electrically heated to  $\pm 0.1\text{ K}$  of the desired temperature by using a controller with a platinum resistance temperature probe (model XMT, produced by Beijing Chaoyang Automatic Instrument Factory).

The sample cell was flushed with ethylene to remove air. A desired amount of the polymer solution was charged into the sample cell. After thermal equilibrium had been reached, ethylene was compressed into the IR cell to the desired pressure. The mixture in the cell was stirred for at least  $2\text{ h}$  using a small magnetic stirrer. The IR spectra at equilibrium were recorded; they were independent of equilibration time. In all cases, the spectrum of P104 in  $p\text{-xylene}$  as background was subtracted.

## Results and Discussion

**Solubilization of Water.** In the previous paper,<sup>21</sup> we showed that the solution of P104 in  $p\text{-xylene}$  could not solubilize water at  $40\text{ }^\circ\text{C}$ , while it could form reverse micelles and solubilize water at  $25\text{ }^\circ\text{C}$ . This can be ascribed to the fact that at the lower temperature  $p\text{-xylene}$  is a selective solvent for the PPO block and thus the copolymer self-assemble to form reverse micelles. However,  $p\text{-xylene}$  is such a good solvent for both

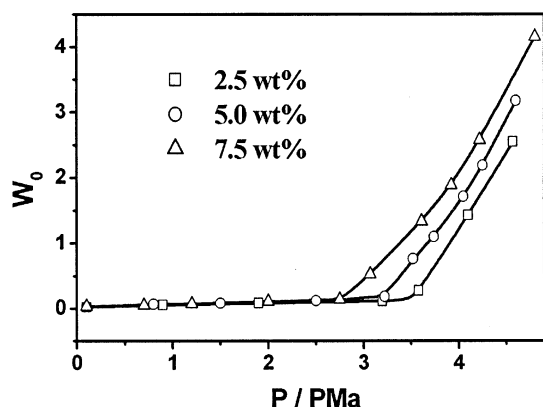


**Figure 2.** Dependence of maximum  $W_0$  on pressure of ethylene and initial concentration of P104 (based on *p*-xylene).

blocks at high temperature that the copolymer cannot assemble to form micelles.<sup>12</sup> However, we observed that the P104 in the CO<sub>2</sub>-expanded *p*-xylene can solubilize water, and the  $W_0$  (the molar ratio of water to EO segments) can be as high as 3.6 under suitable conditions,<sup>21</sup> which is greater than the 1.5–2.0 water molecules required to hydrate a EO group.

Compressed ethylene is soluble in organic solvents and reduces the solvent quality. We expect that the addition of ethylene may also induce the aggregation of P104 in *p*-xylene. Figure 2 shows the maximum  $W_0$  as a function of ethylene pressure at 40.0 °C for the solutions of different P104 concentrations. Maximum  $W_0$  stands for the maximum number of water that each EO segment can solubilize. The trace amount of water dissolved in the solvent (*p*-xylene/ethylene) has been corrected, although it is less than 2% of the total water solubilized. The corrected  $W_0$  is calculated from

$$W_0 = \frac{(m_w - m_{w,0})/M_w}{54m_p/M_p} \quad (1)$$

where  $m_w$  is the total mass of water,  $m_{w,0}$  stands for the mass of water dissolved in the solvent at the experimental temperature and pressure,  $M_w$  is the molar mass of water,  $m_p$  denotes the mass of the surfactant, and  $M_p$  is the molecular weight of P104.

It can be seen from Figure 2 that, comparing with the value at the higher pressures, the maximum  $W_0$  is very small as ethylene pressure is low. This shows that reverse micelles are not formed without ethylene or at the lower pressures. It is interesting that in each curve there is a pressure where maximum  $W_0$  increases sharply with increasing pressure, indicating the reverse micelles begin to form. We define this pressure as a critical micelle pressure (CMP). As expected, the CMP decreases with the concentration of the copolymer. The CMP for the solutions of 2.5, 5, and 7.5 wt % are 3.58, 3.22, and 2.75 MPa, respectively. The maximum  $W_0$  can reach 4.2 under suitable conditions, which means that one polymer molecule can solubilize about more than 400 water molecules. This indicates that reverse micelles are formed and there are water domains in the reverse micelles, which is further proved by the solubilization of MO, a solvatochromic probe, and SAXS and FTIR studies.

The amount of the solubilized water is a function of ethylene pressure, which is easily controlled. As expected, the solubilized water can precipitate after decompression, and solubilization occurs again under

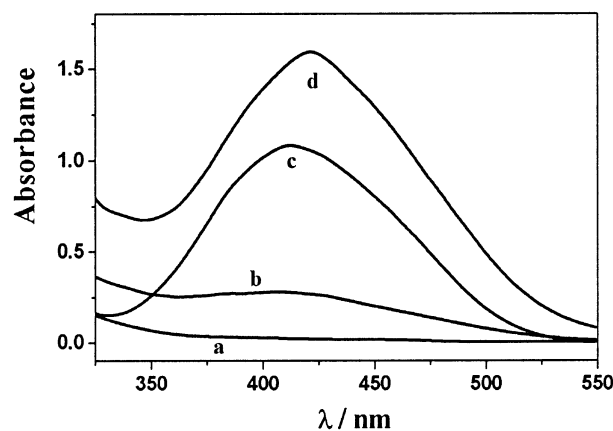


**Figure 3.** UV spectra of MO in different solutions (a: P104/H<sub>2</sub>O/ethylene/*p*-xylene, MO/P104/ethylene/*p*-xylene, MO/H<sub>2</sub>O/ethylene/*p*-xylene, and MO/P104/H<sub>2</sub>O/*p*-xylene; b–d: MO/P104/H<sub>2</sub>O/ethylene/*p*-xylene; the concentration of P104 is 7.5 wt % based on *p*-xylene. b: [MO] =  $2.9 \times 10^{-5}$  M,  $P = 3.01$  MPa,  $W_0 = 0.51$ ,  $\lambda_{\max} = 405$  nm; c: [MO] =  $1.0 \times 10^{-4}$  M,  $P = 3.62$  MPa,  $W_0 = 1.29$ ,  $\lambda_{\max} = 410$  nm; d: [MO] =  $1.5 \times 10^{-4}$  M,  $P = 4.58$  MPa,  $W_0 = 3.52$ ,  $\lambda_{\max} = 428.5$  nm).

ethylene pressure. Thus, the formation and breaking of the reverse micelles can be repeated easily by controlling the pressure, which provides a special advantage for the applications of the reverse micelles formed by this method.

**Solvatochromic Probe Studies.** MO is a useful ionic probe to test the environmental polarity of reverse micelles.<sup>25–28</sup> Its absorbance maximum ( $\lambda_{\max}$ ) shifts toward longer wavelength as the polarity of the environment increases. To confirm that water domains exist and to characterize their properties, a solvatochromic probe study was carried out by UV–vis spectroscopy using MO as a probe.

The absorbance profiles of MO under some typical conditions are illustrated in Figure 3. The solubility of MO in *p*-xylene is extremely low, and the absorption band of MO cannot be observed in the absence of any of the three additives: H<sub>2</sub>O, P104, and suitable pressure of ethylene (Figure 3, curve a). However, the absorption band of MO in the MO/P104/H<sub>2</sub>O/ethylene/*p*-xylene system can be observed as shown in curves b–d, indicating the solubilization of MO. As expected  $\lambda_{\max}$  increases with  $W_0$  because the polarity of the environment of the solubilized MO increases with  $W_0$  (curves b–d). The  $\lambda_{\max}$  at  $W_0 = 0.51$ , 1.29, and 3.52 are 405, 410, 428.5 nm, respectively. The  $\lambda_{\max}$  of MO in pure water determined is 464 nm. These results suggest that the polarity of the environment of the solubilized MO is lower than that of the bulk water, which was also discussed for other reverse micelles.<sup>27,28</sup>

**SAXS Study.** SAXS is one of the most definitive proofs of the formation of micelles.<sup>29,30</sup> Even at high copolymer concentrations, the supramolecular formation of large aggregates and gellike structures can be characterized by scattering techniques.<sup>10</sup> In this work, the reverse micelle system of H<sub>2</sub>O/P104/ethylene/*p*-xylene was studied by SAXS to determine the structures of the micelles. As an example, Figure 4 shows the slit-smeared SAXS spectrum obtained from the reverse micelle system containing 7.5 wt % P104 at 4.8 MPa, and the  $W_0$  is 4.1. There is a sharp peak at  $q = 0.31$  nm<sup>−1</sup>, and a second-order peak at  $q = 0.62$  nm<sup>−1</sup> can be observed. The 1:2 pattern is an indication of lamellar structure.<sup>31–33</sup> The periodicity,  $d$ , of the lamellar struc-



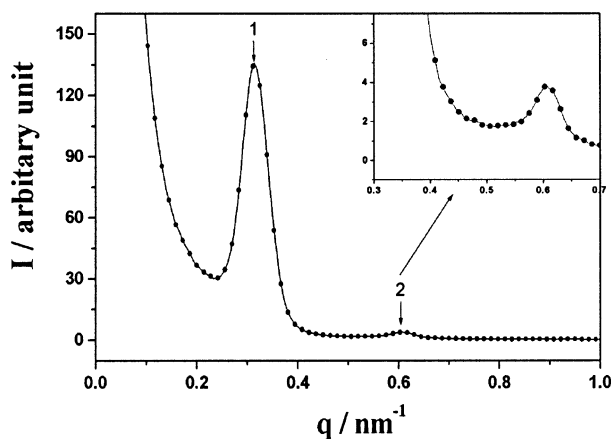


**Figure 4.** Slit-smeared SAXS spectrum obtained from the reverse micelle system of H<sub>2</sub>O/P104/*p*-xylene/ethylene ( $W_0 = 4.1$ ,  $P = 4.8$  MPa; the concentration of P104 in *p*-xylene is 7.5 wt %).

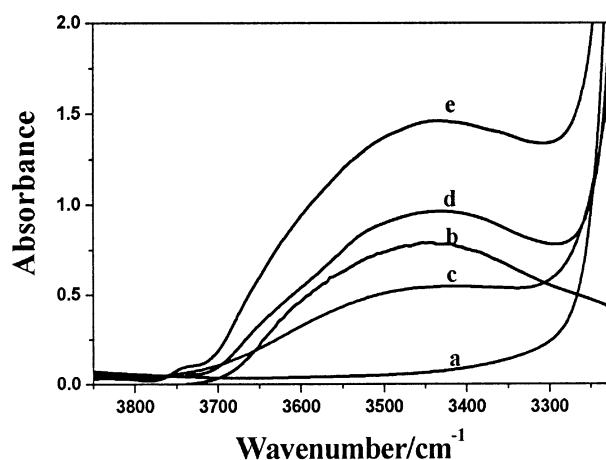


**Figure 5.** FTIR spectra in the  $\nu(\text{O-H})$  region: spectrum a, *p*-xylene/ethylene ( $P = 4$  MPa); spectrum b, thin film of liquid water; spectrum c, H<sub>2</sub>O/P104/*p*-xylene/ethylene ( $W_0 = 0.53$ ,  $P = 3.10$  MPa); spectrum d, H<sub>2</sub>O/P104/*p*-xylene/ethylene ( $W_0 = 1.86$ ,  $P = 3.93$  MPa); spectrum e, H<sub>2</sub>O/P104/*p*-xylene/ethylene ( $W_0 = 3.54$ ,  $P = 4.62$  MPa). The concentration of P104 is 7.5 wt % for spectra c–e.

ture can be determined by the position of the first-order quasi-Bragg peak,  $q_1$ , as  $d = 2\pi/q_1$ .<sup>33</sup> The observed  $d$  increases with the increasing of  $W_0$ . The  $d$  is respectively 17.1, 18.4, and 20.0 nm as  $W_0$  is 1.6, 2.9, and 4.1. The main reason is that the reverse micelle is swollen and the lamellar spacing increases with increasing  $W_0$ .

**FTIR Studies.** Several features of FTIR spectroscopy make it particularly suitable for the study of microemulsions. FTIR is noninvasive, functional group selective, and sensitive to chemical environments, particularly for the detection and characterization of water.<sup>34</sup> It has been widely used to study the structure of reverse micelles and W/O microemulsions.<sup>35,36</sup>

Figure 5 shows the FTIR spectra under different conditions. The FTIR spectrum of liquid water is characterized by a broad O–H stretching absorption ( $\nu(\text{O-H})$ ) in the region of 3750–3100 cm<sup>−1</sup> where the width of the band indicates the presence of many different hydrogen-bonded environments (spectrum 5b). The FTIR spectrum of ethylene in the region of 2800–3400 cm<sup>−1</sup> reveals a broad band centered at ca. 3100 cm<sup>−1</sup> (spectrum 5a). The FTIR spectrum obtained from the microemulsion system of H<sub>2</sub>O/P104/*p*-xylene/ethylene shows the broad feature centered at ca. 3450 cm<sup>−1</sup>,

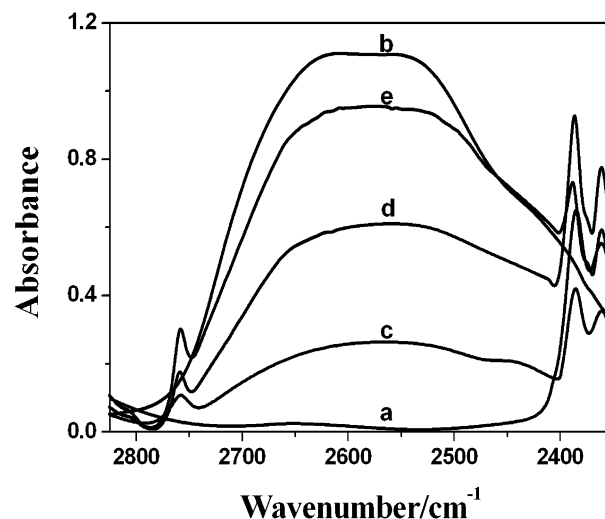


**Figure 6.** FTIR spectra in the  $\nu(\text{O-D})$  region: spectrum a, pure ethylene ( $P = 5$  MPa); spectrum b, liquid film of pure D<sub>2</sub>O; spectrum c, D<sub>2</sub>O/P104/ethylene/*p*-xylene ( $W_0 = 0.53$ ,  $P = 3.10$  MPa); spectrum d, D<sub>2</sub>O/P104/ethylene/*p*-xylene ( $W_0 = 1.86$ ,  $P = 3.93$  MPa); spectrum e, D<sub>2</sub>O/P104/ethylene/*p*-xylene ( $W_0 = 3.54$ ,  $P = 4.62$  MPa). The concentration of P104 is 7.5 wt % for spectra c–e.

which corresponds to the  $\nu(\text{O-H})$  mode of bulk water solubilized in the microemulsion environment.<sup>37–39</sup> This broad band can be assigned to highly hydrogen-bonded water in the microemulsion core, because the O–H stretching frequency is known to decrease in proportion to the hydrogen bond energy.<sup>3</sup>

The increase in mass from H to D causes the bands associated with D<sub>2</sub>O to shift to lower wavenumber. Therefore, we have also studied the FTIR spectra of D<sub>2</sub>O, which are shown in Figure 6. Spectrum a is for pure ethylene at 5 MPa, which shows no strong band in the range of 2800–2400 cm<sup>−1</sup>. Spectrum b is for liquid film of pure D<sub>2</sub>O, which shows the broad  $\nu(\text{O-D})$  feature centered at 2550 cm<sup>−1</sup>. Spectra c–e are for the microemulsion system of D<sub>2</sub>O/P104/ethylene/*p*-xylene at different conditions, which show the broad  $\nu(\text{O-D})$  band of bulk D<sub>2</sub>O. Figure 6 also shows that the absorption maximum of the band of bulk water depends strongly on the amount of water ( $W_0$ ) present. The shoulder peak at ca. 2760 cm<sup>−1</sup> is the spectrum of free D<sub>2</sub>O dissolved in the solvent.<sup>3,37</sup> Therefore, the peak cannot be observed in the spectrum of pure D<sub>2</sub>O (spectrum b).

**Possible Mechanism** A P104 molecule contains 54 hydrophilic EO groups and 61 hydrophobic PO groups, which makes it possible to form reverse micelles. However, the polymer cannot form reverse micelles in *p*-xylene in the absence of ethylene at 40.0 °C. Generally, the micellization of a block copolymer in organic solvents is enthalpy driven.<sup>12,40,41</sup> The standard enthalpy of micellization,  $\Delta H^\circ$ , and the standard entropy of micellization,  $\Delta S^\circ$ , are both negative. Thus, the transfer of the copolymer from solution to reverse micelle (and the subsequent elimination of unfavorable PEO–solvent interactions and replacement of PEO–PEO interacting by favorable PEO–PEO interactions) is exothermic process,<sup>12,40,41</sup> which is disfavored by an increase of temperature. On the other hand, *p*-xylene is a better solvent for the both blocks of the copolymer at higher temperature, and thus the  $\Delta H^\circ$  will be less negative, which also disfavors the micellization. A higher temperature makes *p*-xylene a better solvent so that the copolymer less prone to associate.<sup>12</sup>

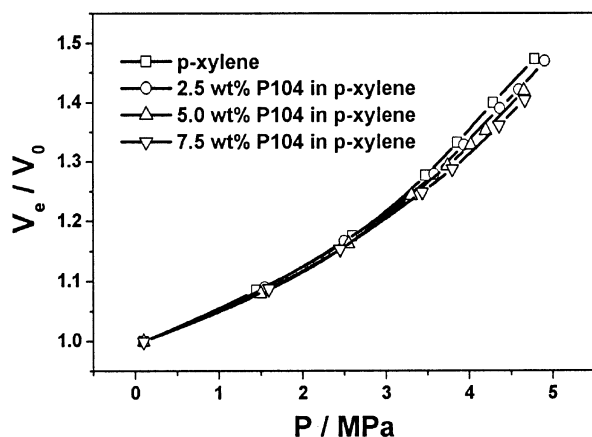


**Figure 7.** Dependence of volume expansion of P104 in *p*-xylene solutions on pressure of ethylene.  $V_e$  is the volume after expansion, and  $V_0$  is the original volume.

Ethylene or  $\text{CO}_2$  is a poor solvent for the polymer, and dissolution of ethylene or  $\text{CO}_2$  will reduce the solvent power of *p*-xylene. Figure 7 shows the volume expansion coefficient of the solutions as a function of the pressure of ethylene. As shown in Figure 7, in the pressure range 3–4.5 MPa, the volume of the solution (copolymer/*p*-xylene) is expanded by 20–40%; i.e., the ethylene has a volume fraction of about 17–30%. As expected, the volume expansion coefficient or the concentration of ethylene in the solutions increases with increasing pressure of ethylene and the solvent power of solvents decreases, as discussed by different researchers.<sup>15,16</sup> When the solvent power decreases, the PEO–solvent interaction will be more unfavorable. So  $\Delta H^\circ$  will be more negative. When the pressure of ethylene is higher than the CMP, the  $\Delta H^\circ$  will be sufficient to outweigh the entropy factor.

As  $\text{CO}_2$  and ethylene are nonpolar and the polarity of PEO is larger than PPO block, the addition of them will have a larger influence on the PEO–solvent interaction. Furthermore, the chain branching will increase the free volume of the PPO and reduce the intermolecular interactions between polymer segments.<sup>42</sup> Thus, PPO will be more soluble in compressed ethylene or  $\text{CO}_2$  than PEO. For example, PPO with a molecular weight of  $1205 \text{ g mol}^{-1}$  has a solubility of 10 wt % in  $\text{CO}_2$  at 35 °C and 20.7 MPa, but PEO with a molecular weight of  $600 \text{ g mol}^{-1}$  has only a solubility of 0.4 wt %.<sup>43</sup> With the addition of compressed ethylene or  $\text{CO}_2$ , the mixed solvent can be tuned to be selective to the PPO block. It is known that block copolymer phases can separate into micelle-like domains when the solvent is selective to one of the blocks.<sup>44,45</sup> Therefore, the copolymers associate to form reverse micelles with a core of PEO coils and a PPO corona at a sufficient concentration of ethylene in the solution.

## Conclusion

The solution of  $(\text{EO})_{27}(\text{PO})_{61}(\text{EO})_{27}$  in *p*-xylene can solubilize a significant amount of water at 40.0 °C as ethylene is dissolved into the solution, although it cannot solubilize a noticeable amount of water in the absence of the gas. The UV spectra indicate that the water domains in the reverse micelles can solubilize MO. SAXS shows lamellar structures in the reverse micellar solution. The FTIR spectra indicate the existence of “bulk” hydrogen-bonded  $\text{H}_2\text{O}$  or  $\text{D}_2\text{O}$  in the core of microdomains, which is distinguishable from the

“free” water dissolved in the solvent. The unique feature of the reverse micelles is that the formation and breaking can be easily controlled by pressure of ethylene. This may have potential applications in many fields, such as chemical reaction engineering, separation science, and nanoparticle preparation.

**Acknowledgment.** The authors are grateful to the National Natural Science Foundation of China (20133030).

## References and Notes

- (1) Laughlin, R. G. *The Aqueous Phase Behavior of Surfactants*; Academic Press: London, 1994.
- (2) Nazario, L. M. M.; Crespo, J. P. S. G.; Holzwarth, J. F.; Hatton, T. A. *Langmuir* **2000**, *16*, 5892.
- (3) Johnston, K. P.; Harrison, K. L.; Clarke, M. J.; Howdle, S. M.; Heitz, M. P.; Bright, F. V.; Carlier, C.; Randolph, T. W. *Science* **1996**, *271*, 624.
- (4) Beckman, E. J. *Science* **1996**, *271*, 613.
- (5) Schwuger, M. J.; Stickdorn, K.; Schomaecker, R. *Chem. Rev.* **1995**, *95*, 849.
- (6) Pillai, V.; Kumar, P.; Hou, M. J.; Ayyub, P.; Shah, D. O. *Adv. Colloid Interface Sci.* **1995**, *55*, 241.
- (7) Nakano, M.; Deguchi, M.; Matsumoto, K.; Matsuoka, H.; Yamaoka, H. *Macromolecules* **1999**, *32*, 7437.
- (8) Alexandridis, P. *Curr. Opin. Colloid Interface Sci.* **1996**, *1*, 490.
- (9) Almgren, M.; Brown, W.; Hvidt, S. *Colloid Polym. Sci.* **1995**, *273*, 2.
- (10) Chu, B. *Langmuir* **1995**, *11*, 414.
- (11) Alexandridis, P.; Andersson, K. *J. Phys. Chem. B* **1997**, *101*, 8103.
- (12) Alexandridis, P.; Andersson, K. *J. Colloid Interface Sci.* **1997**, *194*, 166.
- (13) Jain, N. J.; Aswal, V. K.; Goyal, P. S.; Bahadur, P. *Colloids Surf. A* **2000**, *173*, 85.
- (14) Wanka, G.; Hoffmann, H.; Ulbricht, W. *Macromolecules* **1994**, *27*, 4145.
- (15) Eckert, C. A.; Barbara, L. K.; Debenedetti, P. G. *Nature (London)* **1996**, *383*, 313.
- (16) McHugh, M. A.; Krukonis, V. J. *Supercritical Fluids Extraction: Principles and Practice*, 2nd ed.; Butterworth-Heinemann: Stoneham, MA, 1994.
- (17) Catchpole, O. J.; Hochmann, S.; Anderson, S. R. J. In *High-Pressure Chemical Engineering*; von Rohr, P. R., Trepp, C., Eds.; Elsevier: Amsterdam, 1996; p 309.
- (18) Gallagher, P. M.; Coffey, M. P.; Krukonis, V. J. *J. Supercrit. Fluids* **1992**, *5*, 130.
- (19) Mawson, S.; Johnston, K. P.; Betts, D. E.; McClain, J. B.; DeSimone, J. M. *Macromolecules* **1997**, *30*, 71.
- (20) Musie, G.; Wei, M.; Subramaniam, B.; Busch, D. H. *Coord. Chem. Rev.* **2001**, *219–221*, 789.
- (21) Zhang, R.; Liu, J.; He, J.; Han, B. X.; Zhang, X. G.; Liu, Z. M.; Jiang, T.; Hu, G. H. *Macromolecules* **2002**, *35*, 7869.
- (22) Li, D.; Han, B. X.; Liu, Z. M.; Liu, J.; Zhang, X. G.; Wang, S. G.; Zhang, X. F. *Macromolecules* **2001**, *34*, 2195.
- (23) Dong, B. Z.; Sheng, W. J.; Yang, H. L.; Zhang, Z. J. *J. Appl. Crystallogr.* **1997**, *30*, 877.
- (24) Xu, Q.; Han, B. X.; Yan, H. K. *J. Phys. Chem. A* **1999**, *103*, 5240.
- (25) Reichardt, C. *Chem. Rev.* **1994**, *94*, 2319.
- (26) McFann, G. J.; Johnston, K. P.; Howdle, S. M. *AIChE J.* **1994**, *40*, 543.
- (27) Hutton, B. H.; Stevens, G. W. *Colloids Surf. A* **1999**, *146*, 227.
- (28) Lay, M. B.; Drummond, C. J.; Grieser, F. *J. Colloid Interface Sci.* **1989**, *128*, 602.
- (29) Fulton, J. L.; Pfund, D. M.; McClain, J. B.; Romack, T. J.; Maury, E. E.; Combes, J. R.; Samulski, E. T.; Desimone, J. M.; Capel, M. *Langmuir* **1995**, *11*, 4241.
- (30) Chu, B.; Hsiao, B. S. *Chem. Rev.* **2001**, *101*, 1727.
- (31) *International Tables for Crystallography*; D. Reidel Publishing Company: Dordrecht, 1983; Vol. A.
- (32) Alexandridis, P.; Olsson, U.; Lindman, B. *Macromolecules* **1995**, *28*, 7700.
- (33) Alexandridis, P.; Olsson, U.; Lindman, B. *J. Phys. Chem.* **1996**, *100*, 280.
- (34) Luck, W. A. P. *Water: a Comprehensive Treatise*; Plenum: New York, 1973; Vol 2.

- (35) Ikushima, Y.; Saito, N.; Arai, M. *J. Colloid Interface Sci.* **1997**, *186*, 254.
- (36) Gonzalez-Blanco, C.; Rodriguez, L. J.; Velazquez, M. M. *Langmuir* **1997**, *13*, 1938.
- (37) Clarke, M. J.; Harrison, K. L.; Johnston, K. P.; Howdle, S. M. *J. Am. Chem. Soc.* **1997**, *119*, 6399.
- (38) Angelo, M. D.; Onori, G.; Santucci, A. *J. Phys. Chem.* **1994**, *98*, 3189.
- (39) Angelo, M. D.; Martini, G.; Onori, G.; Ristori, S.; Santucci, A. *J. Phys. Chem.* **1995**, *99*, 1120.
- (40) Alexandridis, P.; Hatton, T. A. In *The Polymeric Materials Encyclopedia*; Salamone, J. C., Ed.; CRC Press: Boca Raton, FL, 1996; Vol. 1, p 743.
- (41) Tuzar, Z.; Kratochvil, P. In *Surface and Colloid Sciences*; Matijevic, E., Ed.; Plenum: New York, 1993; Vol. 15.
- (42) Kirby, C. F.; McHugh, M. A. *Chem. Rev.* **1999**, *99*, 565.
- (43) O'Neill, M. L.; Cao, Q.; Fang, M.; Jonhston, K. P.; Wilkinson, S. P.; Smith, C. D.; Kerschner, S. P.; Jureller, S. H. *Ind. Eng. Chem. Res.* **1998**, *37*, 3067.
- (44) Vagberg, L. J. M.; Cogan, K. A.; Gast, A. P. *Macromolecules* **1991**, *24*, 1670.
- (45) Riess, G.; Hurtrez, G.; Bahadur, P. In *Encyclopedia of Polymer Science & Engineering*, 2nd ed.; Mark, H. F., Bikales, N. M., Overberger, C. C., Menges, G., Eds.; Wiley-Interscience: New York, 1985; Vol 2, p 324.

MA021444D